be employed. Any fixed allocation of Doppler frequency to the two paths will result in errors in T which could reach 100 percent or more.

It is not clear whether the continuing studies will make it possible to determine, from the Pioneer data, credible results of sufficient accuracy to be of significance in the study of Jupiter's atmosphere. However, certain of the problems illustrate the importance of designing spacecraft radio systems with prior consideration of their potential use in radio experiments. Important progress is being made, but much remains to be done (*13*). Continual improvements are important in related measurement, analysis, and theoretical efforts to help realize the potential of such experiments. In addition, other details can have profound effects on accuracy. For example, Eq. 7 shows that for vertical occultations or occultations near the equator or pole, oblateness uncertainties would cause only second-order errors (*14*).

It must be concluded that the apparent agreement of the published T-p profiles for Pioneer 10 and Pioneer 11 was fortuitous since they contain magnified errors due to several different sources. It is possible that appreciable uncertainty will remain after final reappraisals of the Pioneer experiment. However, the radio occultation technique has not yet reached any known fundamental limitation to its potential for accuracy and resolution in the study of any planetary atmosphere. Significant progress toward this ultimate capability is feasible for future missions (*13*).

VON R. ESHLEMAN

Center for Radar Astronomy,
Stanford University,
Stanford, California 94305

References and Notes

1. A. Kliore, G. Fjeldbo, B. L. Seidel, T. T. Sesplaukis, D. W. Sweetnam, P. M. Woiceshyn, *Science* **188**, 474 (1975); A. Kliore, D. L. Cain, G. Fjeldbo, B. L. Seidel, S. I. Rasool, *ibid.* **183**, 323 (1974).
2. A. P. Ingersoll, G. Münch, G. Neugebauer, D. J. Diner, G. S. Orton, B. Schupler, M. Schroeder, S. C. Chase, R. D. Ruiz, L. M. Trafton, *ibid.* **188**, 472 (1975); L. Wallace, M. Prather, M. J. S. Belton, *Astrophys. J.* **193**, 481 (1974).
3. W. B. Hubbard, D. M. Hunten, A. Kliore, *Geophys. Res. Lett.* **2**, 265 (1975).
4. Oblateness was derived from atmospheric results (*1*) but was not used in the program for obtaining these results (*3*).
5. Oblateness can also affect ionospheric profiles, but to a lesser degree. However, it was included (G. Fjeldbo, personal communication) in the derivation of these profiles; G. Fjeldbo, A. Kliore, B. Seidel, D. Sweetnam, D. Cain, *Astron. Astrophys.* **39**, 91 (1975).
6. Past occultation results for Mars and Venus are not expected to have significant errors of the type being discussed for Jupiter, primarily because of the tenuous atmosphere of Mars, the small (undetected) oblateness of Venus, the apparent equipment stability, the relatively small aberration in two-way measurements, and the correspondence of results for Venus with those from in situ measurements.
7. V. R. Eshleman, *Planet. Space Sci.* **21**, 1521 (1973).
8. For large Δ not proportional to M^{-1}, T_f and p_f should be viewed as "pulling" values, with the actual false profile "lagging" behind this pull progressively more with greater depth. The lag is due to the fact that local atmospheric temperature depends on molecular concentrations at all greater heights, so that several scale heights are needed to adjust to changes in T_f. There is a small compensating effect for very dense atmospheric regions, since M then becomes larger than the value given in Eqs. 3 and 4 whereas S stays the same. These effects do not cause a major change in the general shape of the profile, as in Fig. 3, but they do mean that that example at depth is actually representative of a Δ of approximately 10 percent. The three-halves power law relationship of Eq. 6 remains representative.
9. The values of λ and D are assumed to be known to the required precision.
10. The character and possible contribution of several ionospheric effects are included in a separate paper (V.R. Eshleman and G.L. Tyler, in preparation).
11. C. F. Hall, *Science* **183**, 301 (1974).
12. This proposed transponder behavior would produce an error of the right sign and character to help reconcile the Pioneer 11 entry profile. The transponder mode was used in this occultation because of effects of Pioneer 10 oscillator changes on measurements in the upper parts of the ionosphere.
13. In the Mariner Jupiter-Saturn missions (1977 launch), for example, radio-science should be enhanced by the use of two coherently related radio frequencies, increased transmitter powers, and radiation-hardened, ultrastable spacecraft oscillators. The transponders would not be used in occultation experiments. Additional improvements were proposed but will not be incorporated because of fiscal limitations. Certain improvements are also being incorporated in the Viking and Pioneer-Venus missions.
14. Conversely, occultations with large values of tan θ might be used to measure oblateness (with the use of mid-latitudes) or local gravity anomalies and differential rotation, if the atmospheric structure were known from probe or other occultation measurements. There is a potential experiment of this type that could be of significance in determining the reason for the apparent resonance of the rotation of Venus with the position of Earth, based on the use of the long occultations (because absorption limits α) in the Pioneer-Venus orbiter mission.
15. I thank G. L. Tyler for his many important comments on the subject of this report; T. A. Croft, G. Fjeldbo, H. T. Howard, and S. I. Rasool for additional help; and W. B. Hubbard, D. M. Hunten, and A. Kliore for a prepublication copy of their paper. This work was supported by the National Aeronautics and Space Administration.

12 May 1975

Spontaneous Fission-Neutron Fission Xenon: A New Technique for Dating Geological Events

Abstract. *A method for dating geological samples which uses fission product xenon in a manner similar to the use of radiogenic argon in the ^{40}Ar-^{39}Ar technique has been developed. The results of stepwise heating experiments for a zircon from the Ahaggar region in the Sahara are compared to the geochronology determined by the rubidium-strontium, uranium-thorium-lead, and potassium-argon dating methods.*

A notable advance in K-Ar dating consists of fast neutron irradiation of a specimen to convert some of the potassium to ^{39}Ar, and subsequent stepwise heating to release ^{39}Ar and ^{40}Ar (*1, 2*). In addition to being inherently more precise (*3*), this method has provided reliable ages even in cases of significant ^{40}Ar loss (*2*) and can directly measure disturbed ages in discordant samples (*4*). We were thus encouraged to try a similar modification of the U-Xe technique (*5*) with the aim of developing a dating method which uses the ratio of spontaneous fission xenon to neutron fission xenon to measure the age of terrestrial samples (*6*).

A zircon was chosen in an initial attempt to evaluate this technique, for two reasons. First, zircons have a relatively high uranium content and have been shown to be fairly retentive for radiogenic helium (*7*). Second, the particular zircon chosen in this study had previously been dated by the well-established U-Th-Pb method (*8, 9*). The sample, 12.1 mg of zircon M4082 ($\sim 10^3$ grains), was placed in an evacuated quartz capsule and irradiated in a thermal neutron flux for 10 hours. A 1-cm length of 1 percent Co-Al wire placed inside the quartz capsule served as a neutron flux monitor. Measurement of the γ-activity in the monitor wire relative to that in a calibrated Co-Al standard gave a value of $10.2 \pm 0.1 \times 10^{16}$ cm^{-2} for the integrated thermal neutron flux. A few days after the irradiation, the sample was transferred to a high-vacuum extraction line attached to the mass spectrometer and heated in steps of 150° from 200° to 1400°C. The gases evolved from the sample at each temperature step were exposed to Ti as it cooled from 800° to 100°C to remove the chemically reactive substances. Xenon was then separated from the remaining noble gases by adsorption on activated charcoal held at Dry Ice temperature, and its isotopic composition was measured using a high-sensitivity mass spectrometer (*10*) with sufficient resolution to separate xenon isotopes from isobaric hydrocarbons. Instrumental mass discrimination was determined by measurements of samples of xenon prepared from air and comparison with the accepted values of Nier (*11*).

From the production mechanisms it can be shown that the ratio of spontaneous fissions to neutron fissions is given by

$$\frac{S}{N} = \frac{^{238}\mathrm{U}\lambda_{sf}/\lambda_\alpha(e^{\lambda_\alpha T} - 1)}{^{235}\mathrm{U}\,\sigma_{235}\,\phi t}$$

where λ_{sf} and λ_α are the spontaneous fission and α decay constants of ^{238}U, σ_{235} is the thermal neutron fission cross section of ^{235}U, and ϕt is the integrated neutron flux. Thus, the fission xenon age for each temperature fraction in terms of measured quantities is given by

$$T = \frac{1}{\lambda_\alpha} \ln \left[1 + \left(\frac{^{235}\mathrm{U}}{^{238}\mathrm{U}}\right)\left(\frac{\lambda_\alpha}{\lambda_{sf}}\right)\left(\frac{S}{N}\right)\sigma_{235}\phi t \right]$$

The isotopic composition was assumed to be a mixture of three components: an atmospheric component, a spontaneous fission component from ^{238}U, and a neutron fission component from ^{235}U. Since seven isotopes were measured, two methods of analysis were available. In the first we used the isotopes ^{129}Xe and ^{130}Xe, which are not produced in significant quantities in the fission process, and subtracted the atmospheric component from the measured isotopic composition. The ratio of any two of the remaining fission isotopes then determined the ratio of the number of spontaneous fissions to the number of neutron fissions from the relation

$$\frac{S}{N} = \frac{Y_n^i - R_{ij}Y_n^j}{R_{ij}Y_s^j - Y_s^i}$$

where Y_s^i and Y_n^i are the absolute spontaneous and neutron fission yields of isotope i, and R_{ij} is the measured ratio of fission xenon in isotope i to that in isotope j. Although ten dates may be determined in this way, this represents only four independent age determinations. In the second method we determined S/N by means of an unweighted least-squares fit (*12*) which analyzed the isotopic composition in terms of the three components. Since all seven isotopes of xenon are used in the fit, this method provides the most precise date.

The dates were calculated using $\lambda_{sf} = 8.62 \times 10^{-17}$ year^{-1}, $\lambda_\alpha = 1.54 \times 10^{-10}$ year^{-1} (*13*), and the absolute spontaneous fission yields of ^{238}U determined by Young and Thode (*14*). It should be noted that if a different λ_{sf} is used our dates are unaltered, because of the relationship between λ_{sf} and the absolute spontaneous fission yields. Other values used in the calculations were: $\sigma_{235} = 563.7$ barns (*15*), $Y_n{}^{136} = 6.83$ percent $= 6.55 + 0.28$ percent from the reaction $^{135}Xe\ (n,\gamma)\ ^{136}Xe$ (*16*). Yields $Y_n{}^{133}$, $Y_n{}^{132}$, and $Y_n{}^{131}$ were corrected for incomplete decay of the xenon precursors and the decay of ^{133}Xe by multiplying the absolute fission chain yields (*17*) by the fractions shown in parentheses in Table 1. Independent yields for these corrections were taken from Wahl *et al.* (*17*) and the half-lives from Lederer *et al.* (*13*).

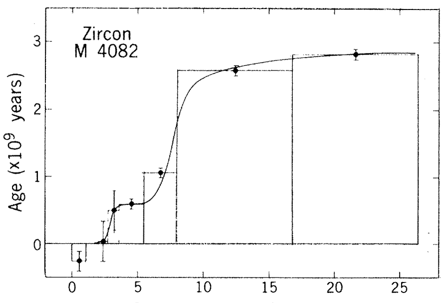

Fig. 1. Spontaneous fission–neutron fission ages versus cumulative fission ^{136}Xe release.

Dates calculated with individual pairs of isotopes were used to check the three-component model for total xenon isotopic composition. The three-component fit was satisfactory for all temperature fractions except that between 650° and 800°C, where a fourth component enriched in ^{131}Xe and ^{132}Xe was present. For this fraction, therefore, the date was calculated using the ratios $^{133}Xe/^{134}Xe$ and $^{133}Xe/^{136}Xe$.

The zircon concentrate, M4082, came from In Ouzzal charnockite in the Sahara. In this general area events at 0.6, 1.1, 1.35, and 2 billion years have been detected by the Rb-Sr, K-Ar, and U-Th-Pb methods. The In Ouzzal formation itself appears to have the following history: primary deposition between 3.3 and 2.9 billion years (*8, 18*) and metamorphism of the granulite facies at 2.05 billion years (*9, 19*). The record of the event at 0.6 billion years is not very clear from normal zircon systematics, even if it is assumed that some granite of this age intruded into the In Ouzzal formation; on the other hand, U-Th-Pb systematics clearly show a recent alteration (*9*).

A plot of the fission xenon age against the cumulative amount of fission ^{136}Xe extracted is shown in Fig. 1. A prominent high-temperature plateau is evident at 2.82 billion years. This date is entirely consistent with the Rb-Sr whole rock age (*18*) and single zircon analysis (*9*). However, this age is detected by the U-Th-Pb method only if zircons are analyzed a single grain at a time and does not appear if the usual method of sampling a zircon population by aggregates of 10^4 to 10^6 grains is used. In this respect, fission xenon dating gives information unobtainable from the usual U-Th-Pb zircon systematics. Less prominent plateaus indicate events at 0.6 and 0 billion years. The latter age was obtained from the lowest-temperature fractions, in which no spontaneous fission xenon was detected, indicating either a very recent loss of spontaneous fission xenon (< 0.1 billion years ago) or a recent incorporation of uranium near the surface of the zircon grains. The plateau at 0.6 billion years is not well defined, but the coincidence with an event at that time affecting the general area from which this zircon was obtained must be pointed out. If further studies confirm these facts it would appear that fission xenon dating has provided a more detailed record of the geological history of this sample than any other method used thus far.

In conclusion, fission xenon dating rep-

Table 1. Dates and xenon isotopic composition (relative to $^{136}Xe = 1.000$) determined by least-squares fit. For ^{131}Xe, ^{132}Xe, and ^{133}Xe, observed fractions of neutron fission chain yields are given in parentheses. Standard deviations of the xenon isotopic composition, except where given, were 3 to 4 percent for the 500° to 650°C temperature step and 1 to 2 percent for the other temperature steps. The 350° to 500°C fraction was lost. Errors given for the ages do not include errors in the absolute fission yields. Abbreviation: STP, standard temperature and pressure.

Temperature fraction (°C)	Extraction time after irradiation (hours)	Age ($\times 10^9$ years)	^{136}Xe ($\times 10^{-11}$ cm^3 STP $\pm$ 15%)	^{134}Xe	^{133}Xe	^{132}Xe	^{131}Xe	^{130}Xe	^{129}Xe
200–350	86.2	-0.26 ± 0.15	1.50	1.188	0.516 (0.676)	1.070 (0.545)	0.753 (0.261)	0.119	0.770
500–650	92.4	0.03 ± 0.30	1.02	1.082	0.441 (0.663)	1.230 (0.569)	0.994 (0.277)	~ 0.2	0.810
650–800	179.7	0.5 ± 0.3*	1.10	1.091	0.2853 (0.438)	1.312 (0.802)	0.776 (0.470)	0.0985	0.677
800–950	182.6	0.59 ± 0.08	1.97	1.144	0.3791 (0.432)	0.677 (0.807)	0.3067 (0.475)	0.0166 ± 0.0004	0.0849
950–1100	186.2	1.06 ± 0.07	2.54	1.116	0.3505 (0.424)	0.605 (0.813)	0.2266 (0.482)	0.0024 ± 0.0002	0.0154
1100–1250	189.5	2.58 ± 0.08	8.81	1.050	0.2504 (0.416)	0.551 (0.819)	0.1716 (0.488)		0.0062 ± 0.0002
1250–1400	192.3	2.82 ± 0.08	9.60	1.039	0.2388 (0.410)	0.550 (0.823)	0.1615 (0.493)		0.0031 ± 0.0001

*Calculated by using $^{136}Xe/^{133}Xe$ and $^{134}Xe/^{133}Xe$; see text.

resents a new and exciting technique for geological dating which can be tested and developed with other examples. The example presented here indicates that the results obtained by this method complement the information obtained by the classical Rb-Sr, U-Th-Pb, and K-Ar methods and that fission xenon dating should prove to be especially valuable for samples that have been affected by a complex series of geological events.

ALBERT TEITSMA
W. B. CLARKE

Department of Physics,
McMaster University,
Hamilton, Ontario, Canada L8S 4K1

C. J. ALLÈGRE

Université Paris VI,
Paris, France

References and Notes

1. C. M. Merrihue, *Trans. Am. Geophys. Union* **46**, 125 (1965).
2. G. Turner, J. A. Miller, R. L. Grasty, *Earth Planet. Sci. Lett.* **1**, 155 (1966).
3. G. B. Dalrymple and M. A. Lamphere, *ibid.* **12**, 300 (1971).
4. V. Stukas and P. H. Reynolds, *ibid.* **22**, 256 (1974).
5. W. A. Butler, P. M. Jeffrey, J. H. Reynolds, G. J. Wasserburg, *J. Geophys. Res.* **68**, 3283 (1963); J. A. Shukolyukov and S. L. Mirkina, *Geochemistry* 7, 729 (1963).
6. A. Teitsma, W. B. Clarke, C. J. Allègre, *Trans. Am. Geophys. Union* **55**, 467 (1974).
7. P. M. Hurley, in *Nuclear Geology*, H. Faul, Ed. (Wiley, New York, 1954), p. 301.
8. C. J. Allègre and R. Caby, *C. R. Hebd. Seances Acad. Sci. Ser. D Sci. Nat.* **275**, 2095 (1972).
9. J. L. Lancelot, A. Vitrac, C. J. Allègre, *ibid.* **277**, 2117 (1973).
10. The instrument is a directional focusing mass spectrometer with a 90° sector, 10-inch radius, and resolution of ~ 625. Maximum sensitivity was achieved by machining the ion beam path out of a solid block of Inconel, which minimizes the internal volume, and by operating the mass spectrometer in the static mode.
11. A. O. Nier, *Phys. Rev.* **79**, 450 (1950).
12. P. K. Davis, R. S. Lewis, J. H. Reynolds, in *Proceedings of the Second Lunar Science Conference*, A. A. Levinson, Ed. (MIT Press, Cambridge, Mass., 1971), vol. 2, p. 1693.
13. C. M. Lederer, J. M. Hollander, L. Perlman, *Table of Isotopes* (Wiley, New York, 1968).
14. B. G. Young and H. G. Thode, *Can. J. Phys.* **38**, 1 (1960).
15. A small correction for epithermal neutrons was made [G. H. Westcott, *At. Energy Can. Ltd. Rep. No. 1101* (1962)].
16. The capture cross section of ^{135}Xe is 3.6×10^6 barns [M. D. Goldberg, S. F. Mughabghab, S. N. Purohit, B. A. Magurno, V. A. May, *Brookhaven Natl. Lab. Rep. No. 325* (1966), vol. IIB].
17. A. C. Wahl, A. E. Norris, R. A. Rouse, J. C. Williams, in *Proceedings of the Second International Atomic Energy Agency Symposium on Physics and Chemistry of Fission* (International Atomic Energy Agency, Vienna, 1969), p. 813.
18. G. Ferrara and M. Gravelle, *Earth Planet. Sci. Lett.* **1**, 319 (1966).
19. C. J. Allègre, R. Caby, M. Tatsumoto, *Trans. Am. Geophys. Union* **53**, 556 (1972).

20. We are grateful to the National Research Council of Canada and the Geological Survey of Canada for grants supporting this work. The mass spectrometer was constructed with funds from an equipment grant awarded by the National Research Council of Canada. We also thank H. D. Howell and J. Cave, who built the mass spectrometer, and E. M. Beaver for his continuous assistance with design and maintenance of electronics and other matters.

10 December 1974; revised 27 January 1975

Supercooling of Water to –92°C Under Pressure

Abstract. *The temperature at which "clean" supercooled water freezes has been determined as a function of pressure up to 3 kilobars, using a differential thermal analysis technique on subdivided water samples. The supercooling limit of such samples, -38° C at normal pressure, is lowered by initial increase of pressure, reaching a minimum value of -92° C at 2.00 kilobars.*

Although water is the most intensively studied of all liquids, there remain important and accessible areas of experimentation in which its properties are quite unknown. The way in which the profoundly anomalous character of liquid water has been emphasized by the recent exploration of the supercooled liquid region at normal pressures (*1–6*) bears testimony to the importance of maximizing the range of pressure and temperature conditions in which measurements are made. Nothing is known of the range over which water can be supercooled under high pressure. To establish the extent of the unexplored pressure-volume-temperature (*PVT*) region for water, we have therefore determined the limit to supercooling at various pressures up to 3 kbar. Our results show that over a considerable range of pressures water can exist as a liquid at temperatures near –90°C, the extent of supercooling being nearly 30°C greater than at 1 atm.

The low temperature limit to supercooling, T_H, is imposed by the onset of homogeneous nucleation (crystal initiation by order fluctuations within the bulk water phase). We determined T_H by means of a simple thermocouple differential thermal analysis technique during cooling of small pressurized samples. The samples, in which heterogeneous nucleation was inhibited by emulsification (*7*), were isolated in thin-walled glass tubes at one end of a ¼-inch stainless steel high-pressure tube, and their thermal behavior was probed using a collinear sample and reference arrangement (*8*) in which the pressure-transmitting fluid served as the reference. To perform a measurement, oil pressure between 1 and 3000 bars was applied to the sample by means of a nonfreezing hydrocarbon fluid and the sample temperature was then lowered at $\sim$3° per minute by inserting the pressure tube plus sample into a glass-jacketed aluminum cylinder 1 inch in diameter, and cooling the assembly in liquid nitrogen. After crystallization was observed the samples were reheated to observe the melting points, T_m, of the ices formed. Differential and total electromotive forces were recorded using a Honeywell two-pen recorder. Results were reproducible to within chart reading uncertainty except at high pressures, where crystallization apparently proceeds rather sluggishly, and some uncertainty in assigning the temperature at which it commences is encountered. Attempts to suppress the crystallization completely, and thus to obtain a vitreous phase of ice directly from the liquid, have not met with success despite the quenching rate of 180° per minute which our small thermal mass system permits.

Results are shown in Fig. 1 for emulsions of water in *n*-heptane and in a mixture of methylcyclohexane (MCH) plus methylcyclopentane (MCP), the latter dispersant phase being necessary for temperatures below the freezing point of *n*-heptane. Some earlier results obtained with a more massive pressure cell and larger samples are included (points denoted under "cell 1" in Fig. 1).

The most significant finding is the very wide region of additional *PTX* space in which properties, *X*, of water can be studied using techniques suitable for the dispersed nature of the sample. It will be possible to investigate somewhat less extensive regions with samples of fine-bore capillary tubes (*1–4*). Use of glass capillary tubing treated to withstand high internal pressure ($\sim$3 kbar) (*9*) should greatly simplify the exploration of this region.

The other striking feature of the results reported here is the similarity between the T_H-pressure function and the equilibrium melting curve. As the melting points of the samples show, the break in the T_H-pressure function is associated with a change in the polymorph of ice being nucleated. The similarity is interesting because homogeneous nucleation is intrinsically a kinetic phenomenon, whereas the triple point at 2.1 kbar and –22°C is determined only by the free energies of ice I, ice III, and water, which become identical at this point. Homogeneous nucleation theory (*10*) shows that the probability of occurrence of order fluctuations large enough to produce viable crystal nuclei in the supercooled liquid increases with increasing difference between the free energies of the solid and liquid. However (*10*) this dependence will lead to a break in T_H at the triple point pressure only if (i) the ice I–water and ice III–water surface free energies are the same and (ii) the probability of order fluctuations in the directions of the two crystal topologies (including fluctuation growth and decay constants) are also equivalent. In binary systems such coincidences are not common, because specific ordering in the liquid often favors fluctuations in the direction of one